

# Chemical Science

rsc.li/chemical-science



ISSN 2041-6539



EDGE ARTICLE

Piet W. N. M. van Leeuwen, Anton Vidal-Ferran *et al.*

XBphos-Rh: a halogen-bond assembled supramolecular catalyst

Cite this: *Chem. Sci.*, 2018, 9, 3644

## XBphos-Rh: a halogen-bond assembled supramolecular catalyst†

Lucas Carreras,<sup>a</sup> Marta Serrano-Torné,<sup>a</sup> Piet W. N. M. van Leeuwen<sup>b</sup> and Anton Vidal-Ferran<sup>a,c</sup>

The use of halogen bonding as a tool to construct a catalyst backbone is reported. Specifically, pyridyl- and iodotetrafluoroaryl-substituted phosphines were assembled in the presence of a rhodium(I) precursor to form the corresponding halogen-bonded complex XBphos-Rh. The presence of fluorine substituents at the iodo-containing supramolecular motif was not necessary for halogen bonding to occur due to the template effect exerted by the rhodium center during formation of the halogen-bonded complex. The halogen-bonded supramolecular complexes were successfully tested in the catalytic hydroboration of terminal alkynes.

Received 15th January 2018  
Accepted 17th February 2018

DOI: 10.1039/c8sc00233a

rsc.li/chemical-science

### Introduction

The evolution of metal-based homogeneous catalysis has run in parallel with the development of structurally diverse ligands.<sup>1</sup> Ligand design allows the behaviour of the metal centre to be influenced and its catalytic activity and selectivity to be modified.

Supramolecular chemistry has emerged as a more efficient tool for the construction of (enantioselective) ligand backbones of metal complexes when compared with standard covalent chemistry. Supramolecular strategies mainly rely on the self-assembly of building blocks that contain both the complementary motifs required for the assembly, and the binding groups necessary for the desired catalysis event. This approach has been successfully employed for preparing catalysts by assembling supramolecularly complementary building blocks through hydrogen-bonding, metal-ligand, or ionic interactions.<sup>2</sup> However, the use of halogen bonding for constructing the backbone of a catalyst remains, to the best of our knowledge, unexplored.<sup>3</sup>

The directionality and strength of halogen bonding,<sup>4</sup> together with a greater tolerance to solvent polarity changes,<sup>5</sup> prompted us to design and develop new halogen-bonded metal catalysts (see Scheme 1). We speculated that the halogen bonding-mediated assembly of two appropriate building

blocks, each bearing a ligating group, could lead to the formation of a metal complex due to the chelation effect that should be exhibited in the presence of the metal centre. With regard to the ligating groups, we focused our attention on phosphino groups due to their pre-eminence in homogeneous catalysis<sup>6</sup> and their tolerance to functionalisation.<sup>7</sup> With respect to the halogen bonding motifs, we envisaged that the use of a fluorinated iodoarene and a pyridine group could be suitable due to the reported complementarity of both supramolecular motifs.<sup>8</sup> Concerning the metal centre, we focused on rhodium as its complexes are catalytically active in pivotal organic transformations. In the discussion that follows, we report our results in the preparation and full characterisation of the first examples of halogen-bonded rhodium(I) complexes and their catalytic performance in alkyne hydroborations.

### Results and discussion

Examination of CPK models revealed that the relative arrangements of the P-ligating groups and the halogen bond acceptor and donor motifs in 2-pyridyldiphenylphosphine (**1**) and 2-iodo-3,4,5,6-tetrafluorophenyldiphenylphosphine (**2**), respectively, were adequate for the formation of the target halogen-bonded Rh(I) complex (see Scheme 2). Building blocks **1** and **2** were

<sup>a</sup>Institute of Chemical Research of Catalonia (ICIQ), The Barcelona Institute of Science and Technology, Av. Paisos Catalans 16, 43007 Tarragona, Spain. E-mail: avidal@iciq.cat

<sup>b</sup>LPCNO, INSA, 135 Avenue de Rangueil, F-31077 Toulouse, France

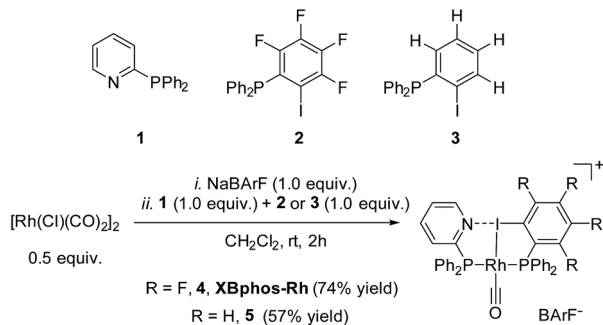
<sup>c</sup>ICREA, Pg. Lluís Companys 23, 08010 Barcelona, Spain

† Electronic supplementary information (ESI) available: Experimental details, spectroscopic and crystallographic data. CCDC 1815870 and 1815871. For ESI and crystallographic data in CIF or other electronic format see DOI: 10.1039/c8sc00233a



Scheme 1 Supramolecular halogen-bonded catalysts (A: halogen bond acceptor; X: halogen bond donor; M: metal centre).





Scheme 2 Synthesis of halogen-bonded rhodium(I) chelates.

successfully prepared in good yields in a multigram scale by slight modification of well-established synthetic protocols.<sup>9</sup> We envisaged that the use of  $[\text{Rh}(\text{Cl})(\text{CO})_2]_2$  along with a halide scavenger would render a putative  $[\text{Rh}(\text{CO})_2]\text{X}$  intermediate that should react with phosphines **1** and **2**. After some experimentation, halogen-bonded rhodium(I) complexes were obtained by first reacting  $[\text{Rh}(\text{Cl})(\text{CO})_2]_2$  and NaBARf,<sup>10</sup> and then adding ligands **1** and **2** as indicated in Scheme 2.<sup>11</sup> The structure of the complex was confirmed by standard spectroscopic studies. The  $^{31}\text{P}\{^1\text{H}\}$  NMR spectrum showed two complex multiplets, from which a high value  $^2J_{\text{P-P}}$  coupling constant (*i.e.* 276 Hz; unequivocally assigned by 2D  $^{31}\text{P}\{^1\text{H}\}$   $J$ -resolved spectroscopy; Fig. SI 52 ESI†) was calculated. According to the literature reviewed, this high value  $^2J_{\text{P-P}}$  coupling constant indicates a *trans*-spanning bisphosphine coordinated to the rhodium centre.<sup>12</sup> We initially expected a dicarbonyl complex, but ESI-MS analysis identified complex  $[\text{Rh}(\text{CO})(\mathbf{1})(\mathbf{2})]\text{BARf}$  (**4**), referred to as XBphos-Rh<sup>13</sup> in the discussion that follows.

X-ray analysis confirmed the proposed halogen-bonded structure of the rhodium complex derived from **1** and **2** (see Scheme 2 for the structure of XBphos-Rh and Fig. 1A for the crystal structure). The nitrogen and iodine are aligned with a N–I distance of 2.757(8) Å and with a  $\text{N}\cdots\text{I}-\text{C}$  bond angle of 169.4(5)°. These structural parameters are in agreement with those reported for halogen-bonded complexes involving pyridine and fluorinated iodoaryl moieties.<sup>14</sup> Interestingly, the iodine appears to be coordinated to the rhodium centre (Rh–I distance = 2.5535(7) Å). Thus, the tridentate coordination of the

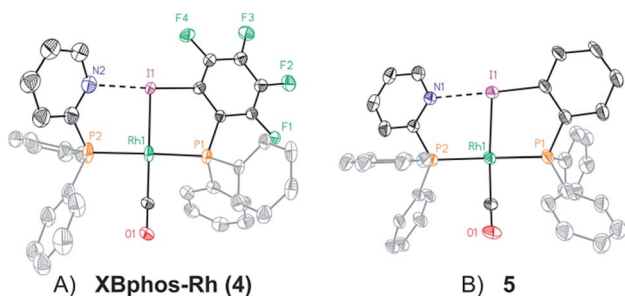


Fig. 1 Crystal structures of XBphos-Rh (A) and **5** (B). Hydrogen atoms and the BARf unit have been omitted for the sake of clarity. Colour scheme: C: black, P: orange, Rh: green, F: green, N: blue, I: purple, O: red. Atomic displacement ellipsoids are drawn at a 50% probability.

halogen-bonded ligands in square planar XBphos-Rh resembles that observed in pincer-type complexes,<sup>15</sup> and therefore this complex can be formally considered as the first reported P–I–P pincer-type complex.

Given the favourable template effect exerted by the rhodium centre on the coordinated atoms in XBphos-Rh, we envisaged that fluorine-free compound **3** could also be used as the halogen bond donor. Thus, complex **5** could be prepared in good yields following a synthetic protocol analogous to that employed for XBphos-Rh (Scheme 2). Crystals from **5** suitable for X-ray analysis confirmed the proposed structure for the rhodium complex derived from **1** and **3** (Scheme 2 and Fig. 1B).

The analysis of the solid-state structures revealed a longer N–I distance for **5** than for XBphos-Rh (2.84(1) Å for **5** and 2.757(8) Å for **4**), which indicates a stronger halogen bond interaction in the fluorine-containing complex.

The formation of a halogen bonding interaction between the pyridine and iodoarene motifs is driven by an enthalpy gain but penalised by an entropic unfavourable contribution arising from the geometry constraints for effective bonding (*i.e.* linear arrangement of the  $\text{N}\cdots\text{I}-\text{C}$  atoms). Overall, the free energy associated with a single interaction is low.<sup>16</sup> In order to gain a deeper insight into the halogen bonding event, full level DFT calculations were carried out. Geometries and stabilities of  $[\text{Rh}(\text{CO})(\mathbf{1})(\mathbf{2})]^+$  and  $[\text{Rh}(\text{CO})(\mathbf{1})(\mathbf{3})]^+$  and those of the starting building blocks were computed with Gaussian 09 (*ref.* 17) with the TPSS<sup>18</sup>-D3<sup>19</sup> density functional employing a medium-sized triple-zeta (def2TZVP<sup>20</sup>) basis set, which is a good compromise between the computational cost and the reliability in describing halogen bonding.<sup>21</sup> Selected geometrical parameters and computed binding free energies are summarised in Table 1. To aid comparison, the supramolecular interaction between 4MePy and IPFB (see footnote *a* in Table 1 for the abbreviations) was also computed and was found to be a slightly endergonic process with a calculated binding constant value being in agreement with that experimentally measured (*i.e.*;  $K_{\text{exp}} = 1 \pm 1 \text{ M}^{-1}$  in toluene in *ref.* 16 and  $K_{\text{calc}} = 0.03 \text{ M}^{-1}$  from the predicted  $\Delta\Delta G$  value in entry 1 in Table 1).

The computed N–I distances were in agreement with the experimental values and their formations were calculated to be highly exergonic processes. Computational studies confirmed a slightly higher stability for  $[\text{Rh}(\text{CO})(\mathbf{1})(\mathbf{2})]^+$  than for  $[\text{Rh}(\text{CO})(\mathbf{1})(\mathbf{3})]^+$  (entries 2 and 3, Table 1). Electrostatic potential surfaces were calculated at the level of theory described above (see Fig. 2 for **2** and  $[\text{Rh}(\text{CO})(\mathbf{1})(\mathbf{2})]^+$  and ESI† for all information). The maximum values of the  $\sigma$ -hole in **2** (Fig. 2) and fluorine-free derivative **3** (ESI†) are 25.1 and 12.5 kcal.mol<sup>−1</sup>, respectively. A lower  $\sigma$ -hole value indicates a lower donor character of the halogen atom to the supramolecular bond. This observation derived from electrostatic potentials is in agreement with previously discussed X-ray data (*i.e.* a longer N–I bond for **5** than for XBphos-Rh).

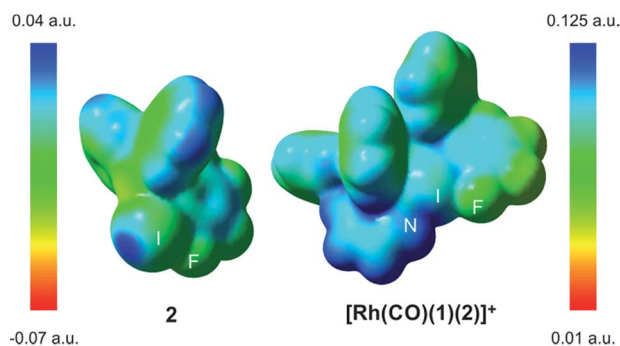
The interesting structural features of XBphos-Rh and **5** (Table 2),<sup>22</sup> prompted us to investigate reactivity features as catalysts that could complement existing catalytic tools. These complexes were tested in the hydroboration of terminal alkynes towards vinylboronic acid derivatives, as the outcome of these



**Table 1** Selected geometrical parameters for halogen-bonded complexes (TPSS-D3/def2TZVP, 298 K, toluene) and computed binding free energies

Entry	Complex	$d_{N-I}$ (Å)	N...I-C bond angle (°)	$\Delta\Delta G$ (kcal·mol <sup>-1</sup> )
1	4MePy·IPFB <sup>a</sup>	2.714	179.4	+2.03 <sup>b</sup>
2 <sup>c</sup>	[Rh(CO)(1)(2)] <sup>+</sup>	2.709 (2.757(8))	175.2 (169.4(5))	-112.83 <sup>d</sup>
3 <sup>c</sup>	[Rh(CO)(1)(3)] <sup>+</sup>	2.827 (2.84(1))	176.2 (171.2(7))	-111.97 <sup>d</sup>

<sup>a</sup> 4MePy·IPFB = complex between 4-methylpyridine and iodopentafluorobenzene. <sup>b</sup>  $\Delta\Delta G = \Delta G_{4MePy-IPFB} - \Delta G_{4MePy} - \Delta G_{IPFB}$ . <sup>c</sup> X-ray values in parentheses. <sup>d</sup>  $\Delta\Delta G = \Delta G_{[Rh(CO)(1)(2 \text{ or } 3)]^+} + \Delta G_{CO} - \Delta G_{[Rh(CO)]^+} - \Delta G_1 - \Delta G_2 \text{ or } 3$ .

**Fig. 2** Electrostatic potential surfaces at an isovalue of 0.001 a.u.

reactions is heavily influenced by the electronic and steric properties of the ligand.<sup>23</sup> Methods for synthesizing vinylboronic acid derivatives, which are important synthetic intermediates, by an atom-economical hydroboration reaction<sup>24</sup> are scarce in the literature.<sup>23,25</sup>

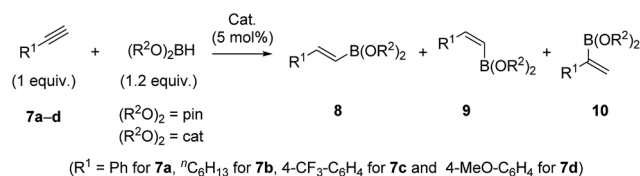
To aid comparison of the results obtained with **XBphos-Rh** and **5**, we included the monodentate [Rh(CO)(PPh<sub>3</sub>)<sub>3</sub>]BARF (**6**) complex in our catalytic studies.<sup>26</sup> A summary of the results obtained is shown in Table 3. Both **XBphos-Rh** and **5** were active hydroboration catalysts, and *E*-isomers **8** were preferentially formed in all cases. Although **XBphos-Rh** is the most selective hydroboration catalyst for phenylacetylene **7a** (88% overall yield for HBpin and 51% for HBcat; entries 1 and 4 in Table 3), hydroboration selectivities for 1-octyne **7b** using **XBphos-Rh** are slightly lower than those with **6** (entries 7–12, Table 3). It is important to mention that in all cases selectivity towards branched derivatives is higher with the halogen-bonded catalysts than with the background catalyst **6**.<sup>26</sup> For example, a ten-fold increase in yield was obtained for the branched product **10a**, pin when **XBphos-Rh** was used (entries 1 and 3, Table 3). It is also noteworthy that, as far as we are aware, **XBphos-Rh**

**Table 2** Selected bond distances (Å) and angles (°)<sup>a</sup>

Entry	Complex	P1–P2	Rh–CO	P1–Rh–P2
1 <sup>b</sup>	[Rh(CO)(xant)]BF <sub>4</sub>	4.506(2)	1.798(5)	164.42(4)
2	<b>XBphos-Rh</b>	4.618(2)	1.872(8)	177.09(7)
3	<b>5</b>	4.632(9)	1.848(9)	178.6(3)

<sup>a</sup> X-ray values. <sup>b</sup> xant = Xantphos; see ref. 22a.

provides the highest reported yield for the branched derivative **10b**, cat (44% branched product with respect to all hydroboration products, entry 10, Table 3). Regarding electronic effects of the product distribution in the hydroboration of aryl-substituted acetylenes, higher ratios of the branched product were obtained for electron-deficient arene **7c** than for electron rich derivative **7d** (entries 13 and 14, Table 3).

**Table 3** Rh-catalysed hydroboration of alkynes<sup>a</sup>

Entry	Alkyne, (R <sup>2</sup> O) <sub>2</sub> BH <sup>b</sup>	Cat.	<b>8 + 9 + 10</b> yield%	Ratio <b>8 : 9 : 10</b>
1 <sup>c</sup>	<b>7a</b> , HBpin	<b>XBphos-Rh</b>	88	78 : 2 : 20 <sup>d</sup>
2	<b>7a</b> , HBpin	<b>5</b>	36	72 : 5 : 23
3	<b>7a</b> , HBpin	<b>6</b>	54	94 : 3 : 3
4	<b>7a</b> , HBcat	<b>XBphos-Rh</b>	51	82 : 2 : 16
5	<b>7a</b> , HBcat	<b>5</b>	49	82 : 2 : 16
6	<b>7a</b> , HBcat	<b>6</b>	50	86 : 9 : 5
7	<b>7b</b> , HBpin	<b>XBphos-Rh</b>	49	79 : 4 : 17
8	<b>7b</b> , HBpin	<b>5</b>	50	79 : 4 : 17
9	<b>7b</b> , HBpin	<b>6</b>	59	93 : 2 : 5
10	<b>7b</b> , HBcat	<b>XBphos-Rh</b>	50	52 : 4 : 44
11	<b>7b</b> , HBcat	<b>5</b>	51	66 : 4 : 30
12	<b>7b</b> , HBcat	<b>6</b>	58	86 : 4 : 10
13 <sup>c</sup>	<b>7c</b> , HBpin	<b>XBphos-Rh</b>	58	71 : 2 : 27
14 <sup>c</sup>	<b>7d</b> , HBpin	<b>XBphos-Rh</b>	74	83 : 3 : 14

<sup>a</sup> Reactions were performed in CD<sub>2</sub>Cl<sub>2</sub> (0.5 M) under N<sub>2</sub> and reacted for 24 h at room temperature. Yields were determined by <sup>1</sup>H NMR using 1,2,4,5-tetramethylbenzene as the internal standard. See ESI<sup>†</sup> for details. <sup>b</sup> (R<sup>2</sup>O)<sub>2</sub>BH: HBpin = pinacolborane, HBcat = catecholborane. <sup>c</sup> 2 equiv. of (R<sup>2</sup>O)<sub>2</sub>BH. <sup>d</sup> Results obtained with bidentate complex [Rh(CO)(Xantphos)]BARF as catalyst in the reaction of **7a** and HBpin are as follows: 69% overall yield (ratio **8 : 9 : 10** = 97 : 2 : 1).

## Conclusions

In summary, we have successfully prepared and fully characterised the first halogen-bonded supramolecular rhodium(i) complexes. To the best of our knowledge, these are the first



examples where halogen bonding is the driving force for the assembly of the catalyst backbone. Furthermore, we have demonstrated that the presence of fluorine groups at the iodo-containing supramolecular motif is not necessary for efficient halogen bonding due to the favourable template effect exerted by the rhodium centre. The two new catalysts are active in the hydroboration of terminal alkynes, with the catalytic activity of **XBphos-Rh** rivalling that of the highest performing catalysts. Moreover, this catalyst favours enhanced ratios of the branched alkenyl boronic acid products. Ongoing investigations in our group include mechanistic studies on the outcome of the reaction,<sup>27</sup> application of this system to other catalytically relevant transformations, extension of the application of this halogen bonding approach to other transition metals, and studies into alternative ligand designs.

## Conflicts of interest

There are no conflicts to declare.

## Acknowledgements

The authors would like to thank MINECO (CTQ2014-60256-P, CTQ2017-89814-P and Severo Ochoa Excellence Accreditation 2014–2018 SEV-2013-0319) and the ICIQ Foundation for the financial support. L. C. thanks MINECO for a FPI-SO predoctoral fellowship (BES-2015-071872). The Université Fédérale Toulouse et Midi-Pyrénées is thanked for an IDEX Chaire d'attractivité. We also thank Dr E. Martin and J. Benet-Buchholz for X-ray crystallographic data, Dr N. Bampos for NMR <sup>31</sup>P{<sup>1</sup>H} *J*-resolved data, Dr J. L. Núñez-Rico for his support with graphic design and Ms R. Somerville for proof reading the manuscript.

## Notes and references

- 1 *Homogeneous Catalysis: Understanding the Art*, ed. P. W. N. M. van Leeuwen, Kluwer Academic Publishers, Dordrecht, 2004.
- 2 For selected reviews, see: (a) B. Breit, *Angew. Chem., Int. Ed.*, 2005, **44**, 6816–6825; (b) A. J. Sandee and J. N. H. Reek, *Dalton Trans.*, 2006, 3385–3391; (c) B. Breit, *Pure Appl. Chem.*, 2008, **80**, 855–860; (d) S. Carboni, C. Gennari, L. Pignataro and U. Piarulli, *Dalton Trans.*, 2011, **40**, 4355–4373; (e) R. Bellini, J. I. van der Vlugt and J. N. H. Reek, *Isr. J. Chem.*, 2012, **52**, 613–629; (f) M. Raynal, P. Ballester, A. Vidal-Ferran and P. W. N. M. van Leeuwen, *Chem. Soc. Rev.*, 2014, **43**, 1660–1733; (g) M. Raynal, P. Ballester, A. Vidal-Ferran and P. W. N. M. van Leeuwen, *Chem. Soc. Rev.*, 2014, **43**, 1734–1787. For a selected example on hydroborations employing supramolecular catalysts, see: (h) S. A. Moteki and J. M. Takacs, *Angew. Chem., Int. Ed.*, 2008, **47**, 894–897.
- 3 For the application of halogen bonding as a secondary interaction for substrate recognition in catalysis, see for example: (a) T. Caronna, R. Liantonio, T. A. Logothetis, P. Metrangolo, T. Pilati and G. Resnati, *J. Am. Chem. Soc.*, 2004, **126**, 4500–4501. For the use of halogen bonding in the stabilisation of the ligand conformation in a metal catalysed transformation, see for example: (b) V. N. G. Lindsay, W. Lin and A. B. Charette, *J. Am. Chem. Soc.*, 2009, **131**, 16383–16385. For the application of halogen bonding in organocatalysis, see for example: (c) D. Bulfield and S. M. Huber, *Chem.–Eur. J.*, 2016, **22**, 14434–14450.
- 4 L. C. Gilday, S. W. Robinson, T. Barendt, M. J. Langton, B. R. Mullaney and P. D. Beer, *Chem. Rev.*, 2015, **115**, 7118–7195.
- 5 M. G. Sarwar, B. Dragisic, L. J. Salsberg, C. Gouliaras and M. S. Taylor, *J. Am. Chem. Soc.*, 2010, **132**, 1646–1653.
- 6 *Phosphorus(III) Ligands in Homogeneous Catalysis: Design and Synthesis*, ed. P. C. J. Kamer and P. W. N. M. van Leeuwen, John Wiley & Sons Ltd., United Kingdom, 2012.
- 7 For examples on the design and use of functionalised phosphorus-based catalysts, see for example: H. Fernández-Pérez, P. Etayo, A. Panossian and A. Vidal-Ferran, *Chem. Rev.*, 2011, **111**, 2119–2176.
- 8 S. Tsuzuki, A. Wakisaka, T. Ono and T. Sonoda, *Chem.–Eur. J.*, 2012, **18**, 951–960.
- 9 For the preparation of **1**, see: (a) P. A. A. Klusener, J. C. L. Suykerbuyk and P. A. Verbrugge, Shell Internationale Research Maatschappij B. V., Eur. Pat. Appl., EP499328A2, 1992. For the preparation of **2** and **3**, see: (b) P. G. Eller and D. W. Meek, *J. Organomet. Chem.*, 1970, **22**, 631–636.
- 10 The tetrakis[3,5-bis(trifluoromethyl)phenyl]borate counterion enhances the solubility and crystallinity of the resulting derivatives, which we deemed as useful for further catalytic studies. See: L. Carreras, L. Rovira, M. Vaquero, I. Mon, E. Martin, J. Benet-Buchholz and A. Vidal-Ferran, *RSC Adv.*, 2017, **7**, 32833–32841.
- 11 Attempts to prepare homocomplexes [Rh(CO)(**1**)<sub>2</sub>]BARF or [Rh(CO)(**2**)<sub>2</sub>]BARF following an analogous strategy to that used for **XBphos-Rh** failed, as complex mixtures of rhodium derivatives were obtained in all cases. Experimental reaction conditions for the selective preparation of rhodium complexes arising from C–I oxidative addition processes in **2** have been also developed (see p. SI-12 in ESI<sup>†</sup>). It is interesting to note that <sup>31</sup>P NMR signals that could correspond to the above mentioned homocomplexes, or complexes arising from C–I oxidative additions in **2**, were not found in any spectra of the crude reaction mixtures.
- 12 Z. Freixa and P. W. N. M. van Leeuwen, *Coord. Chem. Rev.*, 2008, **252**, 1755–1786.
- 13 XB in **XBphos-Rh** stands for halogen (X) bonding (B).
- 14 V. Vasylyeva, L. Catalano, C. Nervi, R. Gobetto, P. Metrangolo and G. Resnati, *CrystEngComm*, 2016, **18**, 2247–2250.
- 15 For representative literature reports on pincer-type metal complexes, see: *Pincer and Pincer-Type Complexes: Applications in Organic Synthesis and Catalysis*, ed. K. J. Szabó and O. F. Wendt, Wiley-VCH, Weinheim, 2014.
- 16 C. C. Robertson, J. S. Wright, E. J. Carrington, R. N. Perutz, C. A. Hunter and L. Brammer, *Chem. Sci.*, 2017, **8**, 5392–5398.



- 17 M. J. Frisch, *et al.*, *Gaussian 09, Revision D.01*, Gaussian, Inc., Wallingford CT, 2013.
- 18 J. Tao, J. P. Perdew, V. N. Staroverov and G. E. Scuseria, *Phys. Rev. Lett.*, 2003, **91**, 146401.
- 19 (a) S. Grimme, J. Antony, S. Ehrlich and H. Krieg, *J. Chem. Phys.*, 2010, **132**, 154104; (b) S. Grimme, S. Ehrlich and L. Goerigk, *J. Comput. Chem.*, 2011, **32**, 1456–1465.
- 20 (a) F. Weigend and R. Ahlrichs, *Phys. Chem. Chem. Phys.*, 2005, **7**, 3297–3305; (b) F. Weigend, *Phys. Chem. Chem. Phys.*, 2006, **8**, 1057–1065.
- 21 R. Sure and S. Grimme, *Chem. Commun.*, 2016, **52**, 9893–9896.
- 22 Examples of ligands with a bite angle close to 180° are scarce in the literature. See, for example: (a) A. J. Sandee, L. A. Van der Veen, J. N. H. Reek, P. C. J. Kamer, M. Lutz, A. L. Spek and P. W. N. M. Van Leeuwen, *Angew. Chem., Int. Ed.*, 1999, **38**, 3231–3235; (b) P. C. J. Kamer, P. W. N. M. van Leeuwen and J. N. H. Reek, *Acc. Chem. Res.*, 2001, **34**, 895–904.
- 23 See, for example: (a) T. Ohmura, Y. Yamamoto and N. Miyaura, *J. Am. Chem. Soc.*, 2000, **122**, 4990–4991; (b) J. Cid, J. J. Carbó and E. Fernández, *Chem.–Eur. J.*, 2012, **18**, 1512–1521.
- 24 These compounds can also be synthesised by hydroboration of alkynes with diboron derivatives. For selected examples, see the following references and those cited therein: (a) H. Jang, A. R. Zhugralin, Y. Lee and A. H. Hoveyda, *J. Am. Chem. Soc.*, 2011, **133**, 7859–7871; (b) D. P. Ojha and K. R. Prabhu, *Org. Lett.*, 2016, **18**, 432–435; (c) B. M. Trost, J. J. Cregg and N. Quach, *J. Am. Chem. Soc.*, 2017, **139**, 5133–5139.
- 25 For selected examples, see the following references and those cited therein: (a) I. D. Gridnev, N. Miyaura and A. Suzuki, *Organometallics*, 1993, **12**, 589–592; (b) S. Pereira and M. Srebnik, *Tetrahedron Lett.*, 1996, **37**, 3283–3286; (c) D. M. Khramov, E. L. Rosen, J. A. V. Er, P. D. Vu, V. M. Lynch and C. W. Bielawski, *Tetrahedron*, 2008, **64**, 6853–6862; (d) N. Iwadate and M. Sugimoto, *Org. Lett.*, 2009, **11**, 1899–1902.
- 26 The bidentate rhodium complex [Rh(CO)(Xantphos)]BARF was also considered a background catalyst in this transformation and incorporated to catalytic hydroboration studies of alkyne **7a** (see footnote *d* in Table 3). [Rh(CO)(Xantphos)]BARF displayed a lower performance than **XBphos-Rh** in terms of overall yield of hydroboration products of **7a** with HBpin.
- 27 As a detailed mechanism on Rh-catalysed hydroboration of terminal alkynes has still to be established (see: B. M. Trost and Z. T. Ball, *Synthesis*, 2005, 853–887), elementary mechanistic steps involving **XBphos-Rh** cannot be unequivocally proposed.

